

AGRICULTURE WASTE TO VALUABLE RESOURCE: COCOA POD HUSK-DERIVED ACTIVATED CARBON (ACCPH) FOR SUSTAINABLE DYE ADSORPTION

Kandlakunta Sumana Mounya¹, Akkina Rajani Chowdary^{2*}

^{1,2*} Department of Microbiology and Food Science & Technology, GITAM School of Science, GITAM (Deemed to be University), Visakhapatnam-530045, Andhra Pradesh, India.

Abstract

The adsorption of industrially significant dyes congo red, xylene fast yellow 2G, anazolene trisodium, direct violet and malachite green onto the activated charcoal derived from cocoa pod husk (ACCPH) in aqueous solution was investigated. The study explored the impact of the amount of adsorbent, pH, contact time and temperature on the adsorption behaviour of these dyes. Notably, it was observed that the adsorption of all dyes on activated charcoal declined with increasing pH and temperature. Adsorption isotherms at different temperatures exhibited an L-type pattern. The experimental data was fittingly analysed using Freundlich, BET, and Langmuir isotherms, allowing the calculation of various adsorption parameters. The optimum temperature for dye adsorption was observed at 298K for 35 minutes with an ACCPH concentration of 0.02g/L.

Thermodynamic parameters, including ΔG , ΔH and ΔS , were computed by examining the linear relationship between $\ln K$ (adsorption coefficient from Langmuir equation) and the reciprocal of temperature ($1/T$). The calculated values for the heat of adsorption and free energy suggested that the adsorption of dyes is more favourable at lower temperatures, and the interaction between the dyes and ACCPH involves chemisorption. These findings provide valuable insights into the adsorption mechanisms and behaviour of these dyes on activated charcoal derived from cocoa pod husk, contributing to understanding sustainable approaches for dye removal from aqueous environments.

Keywords: Adsorption; Cocoa pod husk; Dyes; Activated charcoal; Adsorption isotherm; Thermodynamics of adsorption.

The global agricultural waste market is projected to witness remarkable growth, reaching USD 28.6 billion by 2029, driven by the demand for sustainable alternatives and the adoption of circular economy principles. Within the spectrum of agricultural waste, there's a notable issue specific to cocoa cultivation – cocoa pod wastage. As cocoa (*Theobroma cacao* L.) is grown alongside coconut (*Cocos nucifera* L.) and areca nut (*Areca catechu* L.), the process of cultivating and processing cocoa beans results in substantial waste materials. For each ton of cocoa beans produced, 10 tonnes of pod husks are discarded as waste, making up 70-80% of the weight of the cocoa. These waste materials, including pod husk (65% - 75%), sweating (9% - 10%), and bean shells (2% - 3%) pose a significant challenge for disposal. The rapid pace of technological advancement has led to a significant increase in industrial, agricultural, and domestic waste generation, which requires efficient disposal mechanisms. However, it is unfortunate that many people still discharge these wastes into nearby water sources such as rivers, lakes, and seas. One of the major contributors to environmental pollution is the textile dyeing process, which

continuously releases contaminants into the ecosystem[1]. The amount of wastewater produced by textile dyeing has consistently increased over the years and has now surpassed 700,000 tonnes annually. This wastewater contains around 10,000 different types of dyes and pigments globally, which is an alarming trend that highlights the pressing need for sustainable solutions to mitigate the escalating environmental impact of dye-related pollution. [2]. An estimated 10–15% of dyes are lost in effluents during the dyeing process, contributing to the distinctive colouration of wastewater [3]. Detectable by its colour, wastewater poses a significant concern for both aquatic organisms and the wider ecosystems that depend on water resources. The control of water pollution is crucial to safeguard the well-being of organisms inhabiting water bodies and to ensure the benefits derived from water resources. Many of the dyes that find their way into water sources pose challenges due to their resistance to decomposition, exacerbating concerns over their carcinogenic properties and potential environmental impact[4]. Addressing the discharge of such persistent and potentially harmful substances is pivotal in managing water pollution and preserving the ecological integrity of aquatic environments[5]. Consequently, the removal of these pollutants from wastewater before their final disposal is of utmost importance.

The techniques employed for colour removal from industrial effluents comprise a spectrum of methods, such as biological treatment, coagulation, flotation, adsorption, oxidation, and hyperfiltration. Among the available removal options, adsorption has risen as one of the most efficient and cost-effective methods for the decolourization of textile wastewater [6]. Various adsorbents have been employed for the removal of diverse materials from aqueous solutions, encompassing substances such as dyes, metal ions, and other organic materials. This repertoire includes perlite [7], bentonite [8], peat [9], fly ash [10], lignite [11], silica gels [12], silica [13], and more.

Activated carbon derived from various sources is widely used as an adsorbent for the removal of diverse materials from aqueous solutions. Its high surface area, microporous structure, and radiation stability make it an effective adsorbent in various industrial processes. The adsorption properties of activated carbon are influenced by factors such as particle size, porosity, ash contents, degree of carbonization, and the method of activation. Due to its high degree of microporosity, one gram of activated carbon has a surface area of over 3,000 m². It is used in more than 2,500 commercial product applications, with most wastewater plants using it to purify water and air leaving a facility [14][15][16][17]. Consequently, it finds extensive application in diverse industrial processes as an adsorbent [18], catalyst, or catalyst support [19].

This research paper presents the results of a study conducted on the adsorption of activated charcoal produced from cocoa pod husk (ACCPH) with five different dyes - Congo Red, Xylene Fast Yellow 2G, Anazolene Trisodium, Direct Violet, and Malachite Green. The utilization of activated charcoal derived from cocoa pod husk showcases a practical example of transforming agricultural waste into a valuable tool for pollution control, waste management, and sustainable development, highlighting the importance of innovative solutions in environmental conservation. The dyes were collected from the industrial production line of a textile manufacturing and dyeing

company. The study explores the adsorption behaviour of these dyes concerning the factors - temperature, pH, and the amount of adsorbent used. The adsorption data was fitted to the Freundlich (Eq. (1)), Langmuir (Eq. (2)), and BET (Eq. (3)) isotherms, and the corresponding adsorption parameters, including K_F , n , K , and V_m , were calculated. This comprehensive analysis provides valuable insights into the interaction dynamics between the activated charcoal and the studied dyes under varying environmental conditions.

$$\log \frac{x}{m} = \log K_F + \frac{1}{n} \log C_S \quad (1)$$

The expression $\frac{x}{m} = K_F * C_S^{1/n}$ represents the Freundlich isotherm equation, where $\left(\frac{x}{m}\right)$ is the amount adsorbed per unit mass of the adsorbate, C_S is the equilibrium concentration, and $\frac{1}{n}$ and K_F are constants. The constant K_F is associated with the degree of adsorption, and n offers a rough estimate of the intensity of the adsorption process. The Freundlich isotherm equation is commonly used to describe the non-ideal and heterogeneous nature of adsorption on surfaces.

$$\frac{C_S}{\frac{x}{m}} = \frac{1}{KV_m} + \frac{C_S}{V_m} \quad (2)$$

$$\frac{\frac{C_S}{C_0}}{\frac{x}{m} \left(1 - \frac{C_S}{C_0}\right)} = \frac{1}{x_m C} + \frac{C-1}{x_m C} \left(\frac{C_S}{C_0}\right) \quad (3)$$

Where $\left(\frac{x}{m}\right)$ is the amount of adsorbate adsorbed per unit mass of adsorbent, C_S is the equilibrium concentration of the adsorbate in the solution, C_0 is the initial concentration of the adsorbate in the solution, x_m is the amount of dye required to form a monolayer over the surface of the adsorbent and C is a constant.

Equations (2) and (3) describe the relationship between the amount of adsorbate adsorbed $\left(\frac{x}{m}\right)$ and the equilibrium concentration (C_S).

Thermodynamic studies are crucial for gaining a comprehensive understanding of the nature of adsorption processes. Thermodynamics provides valuable insights into the energetics and spontaneity of adsorption reactions. Key thermodynamic parameters, such as Gibbs free energy change (ΔG), enthalpy change (ΔH), and entropy change (ΔS), are particularly useful in elucidating the underlying mechanisms of adsorption. These parameters can reveal whether the adsorption is a spontaneous or non-spontaneous process, as well as provide information about the stability and feasibility of the adsorption phenomenon under different conditions.[20][21]

Gibbs Free Energy Change is given by the equation:

$$\Delta G = -RT \ln K \quad (4)$$

Where ΔG is Gibbs free energy change, R is the gas constant, T is the temperature (Kelvin), and K is the equilibrium constant.

Van't Hoff Equations are given as

$$\ln K = \frac{\Delta S}{R} - \frac{\Delta H}{RT} \quad (5)$$

$$\Delta G = \Delta H - T\Delta S \quad (6)$$

Where $\ln K$ is the natural logarithm of the equilibrium constant, ΔS is the entropy change, ΔH is the enthalpy change, ΔG is the Gibbs free energy change, R is the gas constant and T is the temperature (Kelvin).

Materials and methods

For the adsorption studies, dyes were sourced from distinct production lines within the textile manufacturing and dyeing industry situated in Rajahmundry. Five different dyes namely Congo Red, Xylene Fast Yellow 2G, Anazolene Trisodium, Direct Violet, and Malachite Green were collected from their respective production line. Each dye was collected from 4 different production lines and further blended to create a homogenous mixture of 2000ml, to facilitate further experimentation. Before experimentation, the collected dyes were validated for confirmation using a spectrophotometer based on their signature wavelength.

A meticulous process is followed to produce activated charcoal from cocoa pod husks. Initially, the husks are carefully cleaned to remove any extraneous materials. Following this, the husks underwent a thorough drying process in a well-ventilated space to reduce moisture content. Subsequently carbonization took place in a controlled environment, subjecting the dried husks to elevated temperatures (480°C–500°C) in the absence of air, transforming them into charcoal. The resulting charcoal was finely ground to increase the surface area, enhancing its adsorption capabilities. Charcoal derived from cocoa pod husks was activated to enhance its adsorption capabilities. For the activation procedure, the ground cocoa pod husk charcoal was subjected to chemical activation using potassium hydroxide (KOH), with a designated charcoal to KOH ratio of 1:5. This mixture was diligently stirred to ensure uniform impregnation of the activating agent. The impregnated charcoal was dried at 473 K (200°C) to remove excess moisture and activate the chemical treatment. Finally, the activated charcoal (ACCPH) was stored in a desiccator to preserve its stability and prevent reabsorption of moisture. The executed process yielded ACCPH with heightened adsorption properties, ready for use in studies involving dye adsorption.

Experimental conditions: All the adsorption experiments were conducted under the following conditions.

Temperature: 298 K, 303 K, 308 K, 313 K, and 318 K.

pH: pH of the solution varied over a range of 1 to 7, including increments of 1 (1, 2, 3, 4, 5, 6, 7)

Amount of adsorbent: 0.005, 0.010, 0.015, 0.020, 0.025, 0.030 grams

Concentration of dyes: anazolene trisodium (7.7 ppm), congo red (3.5 ppm), malachite green (4.6 ppm), direct violet (2 ppm), and xylene fast yellow (4 ppm)

Contact time: 5,10, 15, 20, 25, 30, 35, 40, 45, 50 minutes.

Adsorption and analytical procedures:

During the adsorption experiments, optimum adsorption factors including the amount of adsorbent (0.005-0.030 g), duration of adsorption (10-50 minutes), temperature (298K to 318K) and pH (1-7) were evaluated. 0.02g of ACCPH was finely crushed and mixed with 25ml of dye solutions in a closed Erlenmeyer flask. To determine the optimal time for adsorption studies, the dye solutions were agitated at 150 RPM along with 0.02g of ACCPH. The mixture was then incubated in a water bath incubator (Hitachi PC-26) for 35 minutes at 298K. To serve as control point, each experiment included a blank test without any adsorbent. After 35 minutes, the shaker was stopped, the solid was removed by centrifugation, and the remaining dye in the solution was analysed using a UV–Vis spectrophotometer (Shimadzu UV-120-01). The optimal time for maximum adsorption efficiency was found to be 35 minutes, based on the results of the experiments performed. The pH of the dye solutions was carefully monitored using a pH meter (Model HM-200) to ensure consistency and accuracy throughout the experiments. The buffer volumes for this study were maintained at 2 ppm. The efficiency of the adsorption was analysed by measuring the absorbance of the filtrate at the respective dye λ_{\max} using a spectrophotometer. These standardized parameters were consistently applied in subsequent adsorption studies to ensure reliability and uniformity. The obtained data, including the amount adsorbed ($\frac{x}{m}$) in mg g^{-1} , was plotted against the equilibrium concentration (C_s) in ppm to generate the adsorption isotherms.

Table 1: Maximum wavelength (λ_{\max}) for each dye

S. no.	Dye	λ_{\max} (nm)
1	Malachite green oxalate	620
2	Anazoline trisodium	571
3	Xylene Fast Yellow 2G	405
4	Congo red	497
5	Direct violet	529

The application of the Beer–Lambert law enabled us to determine the remaining concentrations of each dye and better understand their adsorption behaviour on ACCPH. [22]

Results and discussions

Effect of time on adsorption studies

The results of adsorption studies showcased a pattern where dye adsorption increased with the extended contact time until it stabilised as depicted in Fig-1. With prolonged contact time, all available binding sites on the activated carbon surface become occupied by the targeted solutes, leading to a decrease in adsorption capacity. In addition, longer contact times may trigger the

desorption of previously adsorbed molecules, reducing the total adsorption capacity. The optimal contact time for achieving equilibrium was identified as 35 minutes. [23]

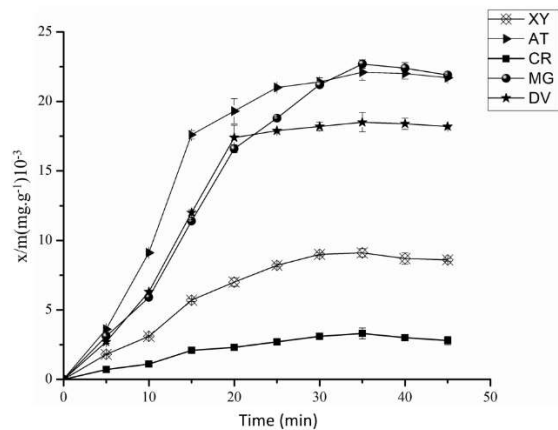


Figure 1: Shaking time vs. adsorption on ACCPH of various dye solutions.

Effect of amount of adsorbent.

After introducing ACCPH at varying concentrations into the dye solutions, the outcomes of the experiments were represented in Fig.2. The observations revealed a discernible trend indicating that the adsorption of dyes increased proportionally with the augmentation of charcoal quantity, reaching a steady state where equilibrium was established. The optimum amount was identified as 0.02 g, a parameter subsequently employed in all subsequent adsorption studies for consistency and reliability in experimental conditions. If the concentration of the adsorbent is excessively high, it can result in the aggregation of adsorbent particles. This aggregation reduces the contact surface area between the adsorbent and adsorbate, which limits the number of active sites available for adsorption. Consequently, this leads to a decrease in the adsorption capacity.

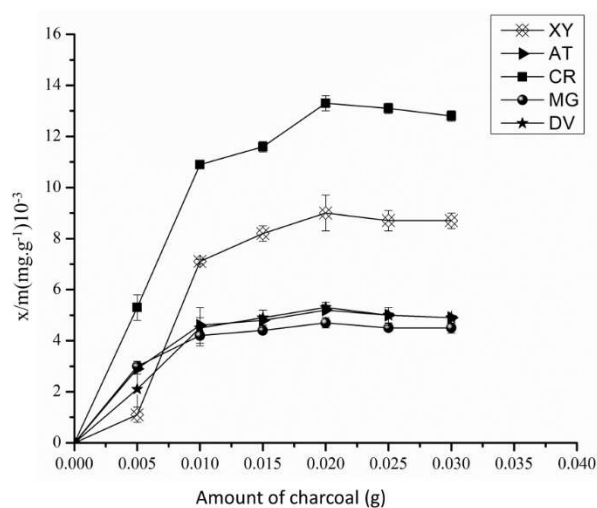


Figure 2: Correlation between adsorbent and adsorbate

Effect of pH of adsorption studies

The concentration of hydrogen ions, also known as pH, has a significant impact on the ionization of dyes and the surface properties of adsorbents [26][27]. Figure 3 shows that the adsorption of most of the selected dyes decreases as the pH increases, except for anazolene trisodium and malachite green on ACCPH. This can be explained by the formation of a positively charged surface on ACCPH. At low pH values, the negative charge on the surface of the charcoal decreases, resulting in an increase in positive charge which enhances the adsorption of negatively charged adsorbates. However, the adsorption of anazolene trisodium and malachite green increases with pH on the surface of ACCPH due to the positive charge exhibited by these dyes and their molecular structures. It is worth noting that a similar study reported the optimal pH value for Anazolene trisodium adsorption to be 13.40 [28].

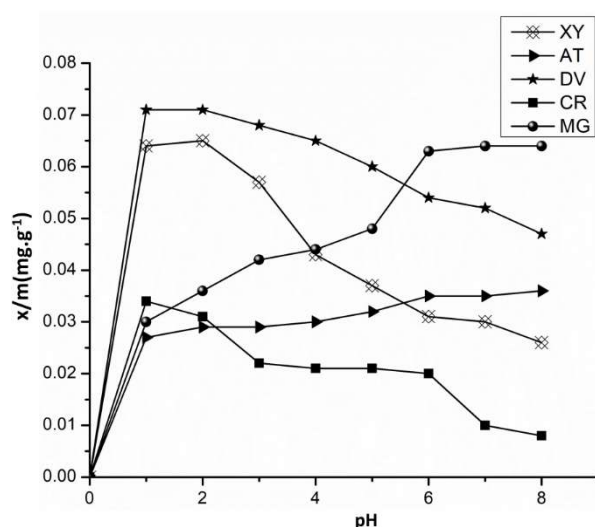


Figure 3: Graphs illustrating the correlation between pH and the quantity of adsorbed dyes at 298 K.

Adsorption isotherms

The systematic acquisition of adsorption isotherms for anazolene trisodium, congo red, malachite green, direct violet, and xylene fast yellow 2G was carried out across temperatures of 298 K, 303 K, 308 K, 313 K, and 318 K. However, only the isotherms at 298 K (24.9 ~ 25°C) are displayed in Fig. 4. These isotherms manifest a distinctive L-type shape, indicating the pronounced affinity of these dyes for ACCPH. The initial adsorption rises sharply with increasing dye concentration, indicating decreased accessibility to vacant sites as more adsorbent sites become occupied. The experimental studies highlight a decrease in adsorption with an increase in temperature, attributed to the exothermic nature of the adsorption process. This phenomenon can also be elucidated by the higher solubility of dyes at elevated temperatures, resulting in a decline in adsorbent-adsorbate interactions and, consequently, a reduction in adsorption. All the examined dyes in this study displayed greater adsorption at the temperature of 298K. These observations resonate with the

findings of a study on the adsorption of orange (IV) and orange G on biopolymer chitin [23][24]. In our case, the adsorption of malachite green similarly decreases with temperature, aligning with results from another research [25].

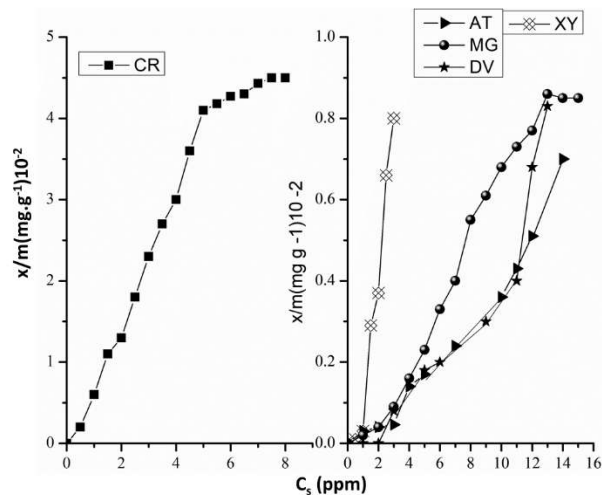


Figure 4: Isothermal adsorption behaviour of different dyes on ACCPH at 298 K

The adsorption data for the dyes on ACCPH were well-described by the linear expression of the Freundlich isotherm (Equation 1), as shown in Figure 5. Table 2 outlines the values of the constants, KF and n. Interestingly, both KF and n decreased with increasing temperature for all dyes, suggesting a preference for adsorption at lower temperatures. For instance, the KF values for congo red ranged from 5 to 8, while for anazolene trisodium, they varied between 4129 and 41583, indicating optimal adsorption at 298K. Higher KF values indicate greater affinity of the dye for the adsorbent. Notably, anazolene trisodium exhibited the highest KF value, highlighting its superior affinity compared to other dyes examined. The 'n' values from Table 2 indicates that the adsorption rate increases slower, than concentration.

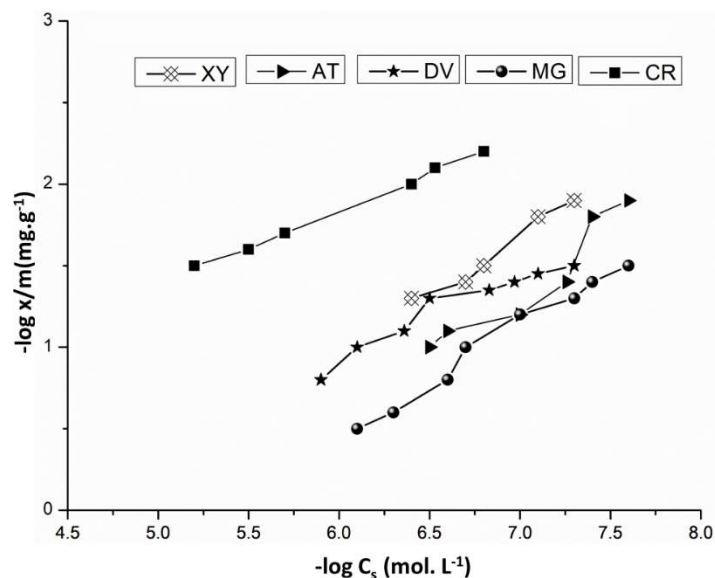


Figure 5: Freundlich adsorption models for different dyes on ACCPH at 298 K.

Table 2: Parameters of the Freundlich Adsorption Model for Different Dyes on ACCPH

Dyes	Temp (K)	n	KF	Correlation coefficient (R ²)
Congo red	298	3.23	8.08	0.9994
	303	2.72	7.91	0.9983
	308	1.95	7.35	0.9847
	313	1.75	6.49	0.9761
	318	1.55	5.17	0.9652
Xylene fast yellow 2G	298	1.54	776.14	0.9853
	303	1.52	647.01	0.9769
	308	1.51	493.11	0.9688
	313	1.5	357.17	0.9607
	318	1.48	24.18	0.9626
Malachite green	298	1.76	548.78	0.9678
	303	1.63	462.16	0.9721
	308	1.57	324.04	0.9764
	313	1.54	224.92	0.9807
	318	1.53	85.82	0.9805
Anazole trisodium	298	1.19	41583.2	0.9769
	303	1.18	29545.21	0.9752
	308	1.15	4834.78	0.9644
	313	1.77	4788.4	0.9581
	318	1.72	4129.85	0.9439
Direct violet	298	1.49	1342.7	0.9873
	303	1.45	1210.41	0.9464
	308	1.49	808.8	0.9481
	313	1.47	597.22	0.9747
	318	1.483	385.64	0.9455

The Langmuir isotherm equation (Equation 2) is observed to be followed by all dyes on ACCPH, as depicted in Figure 6. The logarithmic equations employed in the adsorption studies of dyes on ACCPH exhibit a high degree of linearity, with correlation coefficients ranging from 0.9439 to 0.9994. The strong fit of the Langmuir isotherm equation to the experimental data may be attributed to the uniform distribution of active sites on the activated carbon surface, aligning with the Langmuir equation's assumption of a homogeneous surface. The calculated values for the adsorption coefficient (K) and the monolayer capacity (V_m), derived from the Langmuir equation, are provided in Table 3.

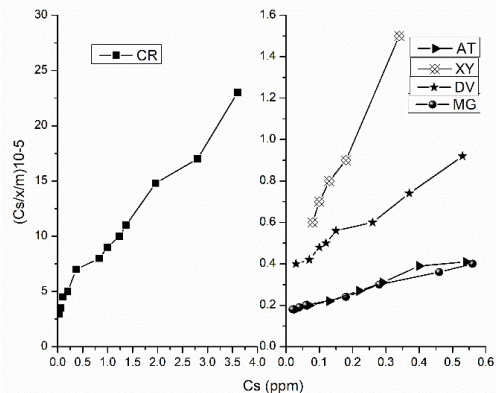


Figure 6: Langmuir Adsorption Behavior of Different Dyes on ACCPH at 298 K

Table 3: Parameters of the Langmuir Adsorption Model for Different Dyes on ACCPH

Dyes	Temperature (K)	K ($\times 10^5$) ($\text{dm}^3 \text{mg}^{-1}$)	Vm (mg g^{-1})	Correlation coefficient (R^2)
Congo red	298	3.85	0.073	0.98690
	303	3.81	0.071	0.99670
	308	2.86	0.069	0.98750
	313	2.34	0.062	0.99097
	318	1.32	0.059	0.99127
Xylene fast yellow 2G	298	30.86	0.09	0.99157
	303	28.65	0.081	0.99187
	308	26.96	0.075	0.99217
	313	21.16	0.06	0.99247
	318	16.86	0.051	0.99277
Malachite green	298	56.74	0.198	0.99307
	303	28.89	0.186	0.99337
	308	19.41	0.183	0.98800
	313	16.68	0.18	0.98930
	318	12.89	0.171	0.97710
Anazolene trisodium	298	530.86	0.197	0.99220
	303	513.23	0.193	0.98675
	308	385.75	0.179	0.98679
	313	258.71	0.173	0.98683
	318	162.73	0.171	0.98687
Direct violet	298	50.62	0.217	0.98691
	303	48.69	0.183	0.99610
	308	29.67	0.179	0.99370

	313	26.52	0.177	0.99750
	318	18.05	0.17	0.97810

The observation indicates that with an increase in temperature, there is a decrease in the values of both K and Vm. Moreover, not all dyes conform to the BET isotherm, suggesting that the adsorption mechanism for all dyes on ACCPH is chemisorption, as illustrated in Figure 7.

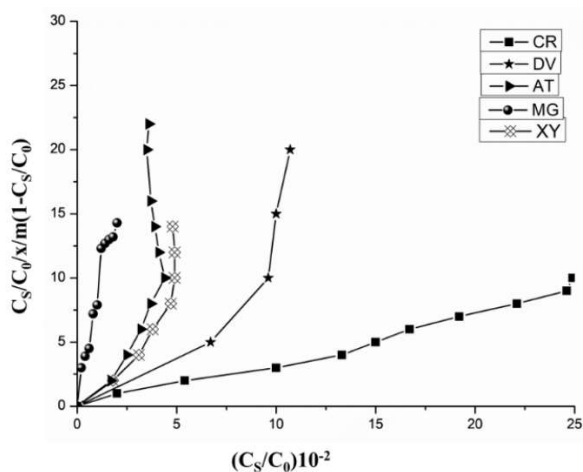


Figure 7: BET Adsorption Isotherms of Dyes at Various Temperatures

Studies on thermodynamic parameters

The calculation of free energy of adsorption was carried out using Equation (4), where "K" represents the adsorption coefficient obtained from the Langmuir equation [29]. The resulting values of free energy are consistently negative across all systems, as presented in Table 4, signifying the spontaneity of the adsorption process. Notably, the ΔG values remain relatively constant for all cases, suggesting that temperature has minimal influence on the free energy of adsorption.

Table 4: Thermodynamic Characteristics of Dye Adsorption onto ACCPH

Dyes	Temperature (K)	$-\Delta G$ (kJ mol ⁻¹)	$-\Delta H$ (kJ mol ⁻¹)	$-\Delta S$ (kJ mol ⁻¹ K ⁻¹)
Congo red	298	32.76	41.34	0.00506
	303	33.52	41.34	0.00429
	308	33.81	41.34	0.00435
	313	32.09	41.34	0.0058
	318	31.75	41.34	0.00573
xylene fast yellow 2G	298	37.41	26.97	0.0408
	303	37.52	26.97	0.0491
	308	37.96	26.97	0.0492

	313	37.85	26.97	0.0484
	318	37.77	26.97	0.0457
Malachite green	298	39.57	56.03	0.0687
	303	38.48	56.03	0.0701
	308	37.04	56.03	0.0709
	313	38.25	56.03	0.0609
	318	37.09	56.03	0.069
Anazolene trisodium	298	44.92	48.13	0.0233
	303	44.59	48.13	0.0109
	308	44.48	48.13	0.0106
	313	44.27	48.13	0.0208
	318	44.01	48.13	0.0235
Direct violet	298	39.2	48.98	0.0447
	303	39.81	48.98	0.0424
	308	39.1	48.98	0.044
	313	38.8	48.98	0.0441
	318	38.75	48.98	0.0442

The heat of adsorption was determined using Equation (5) through the plotting of a graph of $\ln(K)$ against the reciprocal of temperature, as depicted in Figure 8. The resulting slope provided the values of the heat of adsorption, detailed in Table 3. The ΔH values for all the systems exhibit negativity, indicating exothermic processes. Consistent findings were reported in the adsorption of ethyl orange, mentanil yellow, and acid blue from aqueous solutions on industrial waste [30]. Specifically, the ΔH values for malachite green, Anazolene trisodium, and congo red surpass 40 kJ mol^{-1} (as shown in Table 4), implying the chemisorption of these dyes [31]. Although the ΔH value for xylene fast yellow 2G is less than 40 kJ mol^{-1} , the BET isotherms confirm the chemisorption of the dye on ACCPH. Additionally, the entropy was calculated using Equation (6), revealing a decrease in the entropy of adsorption of molecules from the solution on the surface, as presented in Table 4.

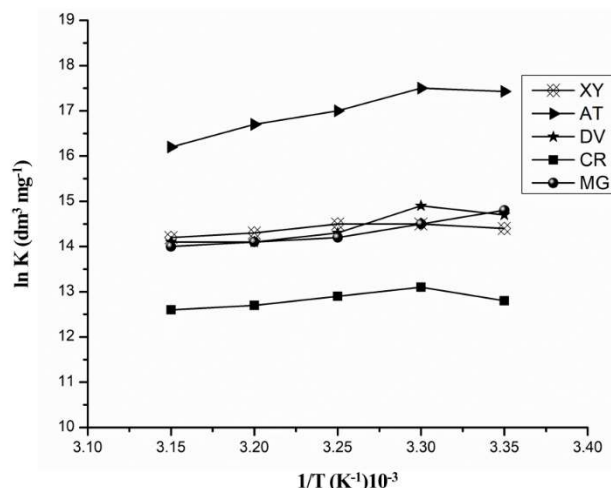


Figure 8: Correlation between $\ln K$ and $1/T$ for the adsorption of different dyes on ACCPH.

Molecules move randomly in a three-dimensional space before they get absorbed onto a surface. Once the absorption takes place, their movement gets restricted towards the surface, which causes a decrease in disorderliness and entropy. However, in the case of xylene fast yellow 2G, there is an increase in entropy observed. The same behaviour was noticed in the adsorption of congo red. Normally, when nonpolar solutes or surfaces come in contact with water, the water structure gets disrupted, and a new, more ordered structure gets imposed on surrounding water molecules. This restructuring of water is generally not favourable for entropy. But, during the adsorption process of xylene fast yellow 2G on the activated carbon surface, the number of water molecules surrounding it decreases. This results in an increase in the degree of freedom of water molecules, which leads to an increased randomness at the solid-solution interface. The positive entropy value indicates this increase in randomness during the adsorption process of xylene fast yellow 2G.

Conclusion

Agriculture plays a fundamental role in global food production, livelihoods, and economic development. However, along with its significance come substantial amounts of waste, ranging from crop residues to processing by-products. Improper management of waste streams can create environmental issues such as pollution and resource depletion. However, agricultural waste, including cocoa pod husk, can be utilized as a valuable resource for waste management and environmental remediation. This presents a promising solution to these challenges.

The use of activated charcoal made from cocoa pod husk (ACCPH) is an effective solution for removing hazardous dyes from water-based solutions. The adsorption isotherms of all the dyes tested showed an L-shape, indicating that ACCPH is a highly effective adsorbent. Additionally, the decrease in adsorption with increasing temperature shows that dye removal using ACCPH is thermodynamically feasible. The optimal temperature for adsorption efficiency is 298K, and the optimal concentration is 0.02g/L, with the removal process taking 35 minutes. It has been observed that the adsorption of dyes on activated charcoal is mainly controlled by chemisorption, as revealed

by the deviation from the BET isotherm for all dyes. This finding indicates that ACCPH exhibits a robust binding affinity for dye molecules. The assertion is further supported by the range of ΔH values (26 to 55 kJ mol⁻¹), which confirms the exothermic nature of the adsorption process. It is worth noting that the way dyes interact with ACCPH changes as the pH level increases. This indicates that the adsorption mechanism is dependent on pH. However, there are some exceptions, like anazolene trisodium and malachite green, which demonstrate unique pH responses. This suggests that the adsorption mechanism may vary depending on the specific dye molecule. Additionally, the negative ΔG and ΔH values affirm the spontaneous and exothermic nature of dye adsorption on ACCPH, further emphasizing its efficacy as an adsorbent for water treatment applications. These findings collectively highlight the promising potential of cocoa pod husk-derived activated charcoal as a sustainable and efficient adsorbent for the removal of hazardous dyes from aqueous environments, offering a viable solution for environmental remediation and pollution control efforts.

References

- 1) Kishor R, Purchase D, Saratale GD, Saratale RG, Gopinath CS, Bilal M, et al. Ecotoxicological and health concerns of persistent coloring pollutants of textile industry wastewater and treatment approaches for environmental safety. *Journal of Environmental Chemical Engineering*. 2021 Apr 1;9(2):105012. Available from: <https://doi.org/10.1016/j.jece.2020.105012>
- 2) Jahan N, Tahmid M, Shoronika AZ, Fariha A, Roy H, Pervez MdN, et al. A Comprehensive Review on the Sustainable Treatment of Textile Wastewater: zero Liquid Discharge and Resource Recovery Perspectives. *Sustainability*. 2022 Nov 19;14(22):15398. Available from: <https://doi.org/10.3390/su142215398>
- 3) AlGarni TS, Al-Mohaimed AM. Water purification by adsorption of pigments or pollutants via metaloxide. *Journal of King Saud University - Science*. 2022 Nov 1;34(8):102339. Available from: <https://doi.org/10.1016/j.jksus.2022.102339>
- 4) Periyasamy AP. Recent advances in the remediation of Textile-Dye-Containing wastewater: prioritizing human health and sustainable wastewater treatment. *Sustainability*. 2024 Jan 5;16(2):495. Available from: <https://doi.org/10.3390/su16020495>
- 5) Yaseen DA, Scholz M. Textile dye wastewater characteristics and constituents of synthetic effluents: a critical review. *International Journal of Environmental Science and Technology*. 2018 Nov 27;16(2):1193–226. Available from: <https://doi.org/10.1007/s13762-018-2130-z>
- 6) Jadhav AC, Jadhav NC. Treatment of textile wastewater using adsorption and adsorbents. In: Elsevier eBooks [Internet]. 2021. p. 235–73. Available from: <https://doi.org/10.1016/b978-0-323-85829-8.00008-0>

- 7) Vassileva P, Tumbalev V, Kichukova D, Voykova D, Kovacheva D, Spassova I. Study on the Dye Removal from Aqueous Solutions by Graphene-Based Adsorbents. *Materials*. 2023 Aug 22;16(17):5754. Available from: <https://doi.org/10.3390/ma16175754>
- 8) Marouf R, Dali N, Boudouara N, Ouadjenia F, Zahaf F. Study of adsorption properties of bentonite clay. In: *IntechOpen eBooks*. 2021. Available from: <https://doi.org/10.5772/intechopen.96524>
- 9) Allen S, McKay G, Porter JF. Adsorption isotherm models for basic dye adsorption by peat in single and binary component systems. *Journal of Colloid and Interface Science*. 2004 Dec 1;280(2):322–33. Available from: <https://doi.org/10.1016/j.jcis.2004.08.078>
- 10) Aigbe UO, Ukhurebor KE, Onyancha RB, Osibote OA, Darmokoesoemo H, Kusuma HS. Fly ash-based adsorbent for adsorption of heavy metals and dyes from aqueous solution: a review. *Journal of Materials Research and Technology*. 2021 Sep 1;14:2751–74. Available from: <https://doi.org/10.1016/j.jmrt.2021.07.140>
- 11) Vrchovecká S, Asatiani N, Antoš V, Waclawek S, Hrabák P. Study of adsorption efficiency of lignite, biochar, and polymeric nanofibers for veterinary drugs in WWTP effluent water. *Water, Air, & Soil Pollution*. 2023 Apr 1;234(4). Available from: <https://doi.org/10.1007/s11270-023-06281-0>
- 12) Chua HT, Ng KC, Chakraborty A, Oo NM, Othman MA. Adsorption characteristics of silica gel + water systems. *Journal of Chemical & Engineering Data*. 2002 Jun 26;47(5):1177–81. Available from: <https://doi.org/10.1021/je0255067>
- 13) Parida SK, Dash S, Patel S, Mishra BK. Adsorption of organic molecules on silica surface. *Advances in Colloid and Interface Science*. 2006 Sep 1;121(1–3):77–110. Available from: <https://doi.org/10.1016/j.cis.2006.05.028>
- 14) Nowicki, (2018), Nowicki, H. (2018, August 2). The basics of activated carbon adsorption. *Water Technology*. <https://www.watertechnonline.com/wastewater/article/15549902/the-basics-of-activated-carbon-adsorption>
- 15) Sarkar & Ahuja, (2022) (Sarkar, S., & Ahuja, S. (2022). Applications and limitations of graphene oxide for remediating contaminants of emerging concern in wastewater. In *Separation Science and technology* (pp. 209–222). <https://doi.org/10.1016/b978-0-323-90763-7.00012-3>
- 16) Ganjoo et al., (2023) (Ganjoo, R., Sharma, S., Kumar, A., & Daouda, M. M. A. (2023). Activated Carbon: Fundamentals, classification, and properties. In *The Royal Society of Chemistry eBooks* (pp. 1–22). <https://doi.org/10.1039/bk9781839169861-00001>
- 17) Saha & Grappe, (2017) (Saha, D., & Grappe, H. A. (2017). Adsorption properties of activated carbon fibers. In *Elsevier eBooks* (pp. 143–165). <https://doi.org/10.1016/b978-0-08-100660-3.00005-5>

- 18) Pendleton P, Wu SH. Kinetics of dodecanoic acid adsorption from caustic solution by activated carbon. *Journal of Colloid and Interface Science* .2003 Oct 1;266(2):245–50. Available from: [https://doi.org/10.1016/s0021-9797\(03\)00575-7](https://doi.org/10.1016/s0021-9797(03)00575-7)
- 19) Wang L, Han Q, Li D, Wang Z, Chen J, Chen S, et al. Comparisons of Pt catalysts supported on active carbon, carbon molecular sieve, carbon nanotubes and graphite for HI decomposition at different temperature. *International Journal of Hydrogen Energy* . 2013 Jan 1;38(1):109–16. Available from: <https://doi.org/10.1016/j.ijhydene.2012.10.052>
- 20) Nugent P, Belmabkhout Y, Burd S, Cairns A, Luebke R, Forrest KA, et al. Porous materials with optimal adsorption thermodynamics and kinetics for CO₂ separation. *Nature*. 2013 Feb 27;495(7439):80–4. Available from: <https://doi.org/10.1038/nature11893>
- 21) Hu R, Wang W, Tan J, Chen L, Dick JM, He G. Mechanisms of shale gas adsorption: Insights from a comparative study on a thermodynamic investigation of microfossil-rich shale and non-microfossil shale. *Chemical Engineering Journal*. 2021 May 1;411:128463. Available from: <https://doi.org/10.1016/j.cej.2021.128463>
- 22) Rajasekhar KK, Babu R, Veena BM, Lavanya G, Haripriya P, Hamsini KV. Adsorption studies of methylene blue and congo red on the surface of *Citrus aurantium*. *Asian Journal of Chemistry*. 2009 Jan 1;21(2):1531–4. Available from: <https://www.cabdirect.org/cabdirect/abstract/20093256349>
- 23) Qiu J, Feng Y, Zhang X, Jia M, Yao J. Acid-promoted synthesis of UiO-66 for highly selective adsorption of anionic dyes: Adsorption performance and mechanisms. *Journal of Colloid and Interface Science*. 2017 Aug 1;499:151–8. Available from: <https://doi.org/10.1016/j.jcis.2017.03.101>
- 24) Chiou M, Ho PY, Li H. Adsorption of anionic dyes in acid solutions using chemically cross-linked chitosan beads. *Dyes and Pigments*. 2004 Jan 1;60(1):69–84. Available from: [https://doi.org/10.1016/s0143-7208\(03\)00140-2](https://doi.org/10.1016/s0143-7208(03)00140-2)
- 25) Jana S, Ray J, Mondal B, Tripathy T. Efficient and selective removal of cationic organic dyes from their aqueous solutions by a nanocomposite hydrogel, katira gum-cl-poly(acrylic acid-co-N, N-dimethylacrylamide)@bentonite. *Applied Clay Science*. 2019 Jun 1;173:46–64. Available from: <https://doi.org/10.1016/j.clay.2019.03.009>
- 26) Suchithra PS, Linsha V, Mohamed A, Ananthakumar S. Mesoporous organic–inorganic hybrid aerogels through ultrasonic assisted sol–gel intercalation of silica–PEG in bentonite for effective removal of dyes, volatile organic pollutants and petroleum products from aqueous solution. *Chemical Engineering Journal* . 2012 Aug 1;200–202:589–600. Available from: <https://doi.org/10.1016/j.cej.2012.06.083>
- 27) Suchithra PS, Linsha V, Mohamed A, Ananthakumar S. Mesoporous organic–inorganic hybrid aerogels through ultrasonic assisted sol–gel intercalation of silica–PEG in bentonite for

effective removal of dyes, volatile organic pollutants and petroleum products from aqueous solution. *Chemical Engineering Journal*. 2012 Aug 1;200–202:589–600. Available from: <https://doi.org/10.1016/j.cej.2012.06.083>

28) Ravikumar K, Deebika B, Balu K. Decolourization of aqueous dye solutions by a novel adsorbent: Application of statistical designs and surface plots for the optimization and regression analysis. *Journal of Hazardous Materials*. 2005 Jun 1;122(1–2):75–83. Available from: <https://doi.org/10.1016/j.jhazmat.2005.03.008>

29) Mittal A, Kurup L, Gupta VK. Use of waste materials—Bottom Ash and De-Oiled Soya, as potential adsorbents for the removal of Amaranth from aqueous solutions. *Journal of Hazardous Materials*. 2005 Jan 1;117(2–3):171–8. Available from: <https://doi.org/10.1016/j.jhazmat.2004.09.016>

30) Jain A, Gupta VK, Bhatnagar A, Suhas S. Utilization of industrial waste products as adsorbents for the removal of dyes. *Journal of Hazardous Materials*. 2003 Jul 1;101(1):31–42. Available from: [https://doi.org/10.1016/s0304-3894\(03\)00146-8](https://doi.org/10.1016/s0304-3894(03)00146-8)

31) Smičiklas I, Smiljanić S, Perić-Grujić A, Šljivić-Ivanović MZ, Mitrić M, Antonović D. Effect of acid treatment on red mud properties with implications on Ni(II) sorption and stability. *Chemical Engineering Journal*. 2014 Apr 1;242:27–35. Available from: <https://doi.org/10.1016/j.cej.2013.12.079>

32) Attia AA, El-Hendawy ANA, Khedr SA, El-Nabarawy Th. Textural Properties and Adsorption of Dyes onto Carbons Derived from Cotton Stalks. *Adsorption Science & Technology*. 2004 Jun 1;22(5):411–26. Available from: <https://doi.org/10.1260/0263617042863075>